Biogeosciences Discuss., 7, 3019–3059, 2010
www.biogeosciences-discuss.net/7/3019/2010/


Biogeosciences Discussions

This discussion paper is/has been under review for the journal Biogeosciences (BG).
Please refer to the corresponding final paper in BG if available.

# Biogeochemical controls and isotopic signatures of nitrous oxide production by a marine ammonia-oxidizing bacterium

**C. H. Frame**[1,2] **and K. L. Casciotti**[1]

[1]Marine Chemistry and Geochemistry, Woods Hole Oceanographic Institution, Woods Hole, Massachusetts, USA
[2]Joint Program in Chemical Oceanography, Massachusetts Institute of Technology/Woods Hole Oceanographic Institution, Woods Hole, Massachusetts, USA

Received: 2 April 2010 – Accepted: 8 April 2010 – Published: 27 April 2010

Correspondence to: C. H. Frame (cframe@whoi.edu)

Published by Copernicus Publications on behalf of the European Geosciences Union.





## Abstract

Nitrous oxide ($N_2O$) is a trace gas that contributes to greenhouse warming of the atmosphere and stratospheric ozone depletion. The $N_2O$ yield from nitrification (moles $N_2O$-N produced/mole ammonium-N consumed) has been used to estimate marine $N_2O$ production rates from measured nitrification rates and global estimates of oceanic export production. However, the $N_2O$ yield from nitrification is not constant. Previous culture-based measurements indicate that $N_2O$ yield increases as oxygen ($O_2$) concentration decreases and as nitrite ($NO_2^-$) concentration increases. These results were obtained in substrate-rich conditions and may not reflect $N_2O$ production in the ocean. Here, we have measured yields of $N_2O$ from cultures of the marine $\beta$-proteobacterium *Nitrosomonas marina* C-113a as they grew on low-ammonium (50 µM) media. These yields were lower than previous reports, between $4 \times 10^{-4}$ and $7 \times 10^{-4}$ (moles N/mole N). The observed impact of $O_2$ concentration on yield was also smaller than previously reported under all conditions except at high starting cell densities ($1.5 \times 10^6$ cells ml$^{-1}$), where 160-fold higher yields were observed at 0.5% $O_2$ compared with 20% $O_2$. At environmentally relevant cell densities ($2 \times 10^2$ to $2.1 \times 10^4$ cells ml$^{-1}$), cultures grown under 0.5% $O_2$ had yields that were only 1.25- to 1.73-fold higher than cultures grown under 20% $O_2$. Thus, previously reported many-fold increases in $N_2O$ yield with dropping $O_2$ could be reproduced only at cell densities that far exceeded those of ammonia oxidizers in the ocean. The presence of excess $NO_2^-$ (up to 1 mM) in the growth medium also increased $N_2O$ yields by an average of 70% to 87% depending on $O_2$ concentration. We made stable isotopic measurements on $N_2O$ from these cultures to identify the biochemical mechanisms behind variations in $N_2O$ yield. Based on measurements of $\delta^{15}N$, site preference ($SP=\delta^{15}N^{\alpha} - \delta^{15}N^{\beta}$), and $\delta^{18}O$, we estimate that nitrifier-denitrification produced between 11% and 26% of $N_2O$ from cultures grown under 20% $O_2$ and 43% to 87% under 0.5% $O_2$. We also demonstrate that a positive correlation between SP and $\delta^{18}O$-$N_2O$ is expected when nitrifying bacteria produce $N_2O$. A positive relationship between SP and $\delta^{18}O$-$N_2O$ has been observed in environmental



BGD

7, 3019–3059, 2010



$N_2O$ datasets, but until now, explanations for the observation invoked only denitrification. Such interpretations may overestimate the role of heterotrophic denitrification and underestimate the role of ammonia oxidation in environmental $N_2O$ production.

## 1 Introduction

The atmospheric concentration of the greenhouse gas nitrous oxide ($N_2O$) has risen steadily over the last century. Processes in the microbial nitrogen cycle are the largest source of atmospheric $N_2O$ and nearly one-third of this may come from the oceans (Nevison et al., 1995). Humans have greatly increased the amount of fixed nitrogen entering the oceans (Galloway et al., 1995), and the functioning of marine microbial ecosystems is shifting in response (Fulweiler et al., 2007; Beman et al., 2005; Naqvi et al., 2000). Understanding the impact of anthropogenic activity on the size of the marine $N_2O$ source requires knowledge of which microbes are involved in $N_2O$ production and how the production is controlled by chemical variables.

Nitrification, and in particular ammonia oxidation, is thought to dominate $N_2O$ production in oxic water columns (Elkins et al., 1978; Cohen and Gordon, 1979; Goreau et al., 1980; Ostrom et al., 2000; Popp et al., 2002). Oversaturations of dissolved $N_2O$ ($\Delta N_2O$, nmol $L^{-1}$) are often positively correlated with apparent oxygen utilization (AOU) (Yoshinari, 1976; Cohen and Gordon, 1978; Elkins et al., 1978). Since AOU is a tracer of organic matter remineralization, the direct relationship between AOU and $\Delta N_2O$ is taken as evidence that $N_2O$ is produced by nitrifying organisms. However, the linear AOU-$N_2O$ relationship breaks down unpredictably in low-$O_2$ environments. Several different factors may contribute to this break-down: 1) at low $O_2$ concentrations, ammonia-oxidizing bacteria produce higher yields of $N_2O$ per mole of $NH_4^+$ oxidized (Goreau et al., 1980; Jorgensen et al., 1984) 2) heterotrophic denitrifying bacteria produce more $N_2O$ in low-$O_2$ conditions (Knowles et al., 1981; Payne et al., 1971) 3) in stably anoxic environments denitrifying bacteria are net consumers of $N_2O$, which they reduce to nitrogen gas ($N_2$) (Cline et al., 1987).



BGD
7, 3019–3059, 2010



There is probably niche overlap among nitrifiers and denitrifiers in low-$O_2$ environments, making it especially difficult to distinguish between these two $N_2O$ sources. Ammonia-oxidizing bacteria are able to thrive at low $O_2$ concentrations (Carlucci and McNally, 1969; Goreau et al., 1980; Codispoti and Christensen, 1985) and it has been suggested that denitrification occurs in oxic ocean waters in the anaerobic interiors of organic particles (Yoshida et al., 1989; Alldredge and Cohen, 1987). However, to understand the individual impacts of these processes on the total marine $N_2O$ budget, we must be able to separate their responses to environmental changes.

Stoichiometric relationships among $N_2O$ production, $NO_3^-$-regeneration, and AOU are also a convenient tool for converting oceanographic nutrient and $O_2$ data to estimates of $N_2O$ production (e.g., Codispoti and Christensen, 1985; Fuhrman and Capone, 1991; Jin and Gruber, 2003; Suntharalingam and Sarmiento, 2000) or using $N_2O$ concentration data to calculate nitrification rates (e.g., Law and Ling, 2001). However, there is not a universal AOU:$N_2O$ ratio; open-ocean AOU:$N_2O$ ratios differ from low-$O_2$ environments (Cohen and Gordon, 1979). $N_2O$ yields based on regressions of oceanographic data are also strongly influenced by mixing gradients, making them unreliable gauges for biological $N_2O$ production (Nevison et al., 2003). Alternative yield estimates are based on measurements of $N_2O$ production by cultures of ammonia-oxidizing bacteria (Goreau et al., 1980). However, these yield estimates may not be applicable to the ocean when they are made using non-representative strains grown at extremely high cell densities in substrate-rich media.

Understanding the nitrification $N_2O$ source is particularly complicated because ammonia oxidizers contain two distinct $N_2O$-producing pathways that may respond differently to geochemical controls. One pathway is the oxidative decomposition of hydroxylamine ($NH_2OH$), or one of its derivatives, during the conversion of $NH_3$ to $NO_2^-$ (Hooper and Terry, 1979). The other mechanism, known as nitrifier-denitrification, is the sequential reduction of $NO_2^-$ to NO and then $N_2O$ by the action of the nitrite reductase (NIR, encoded by the gene *nirK*) and the nitric oxide reductase (NOR, encoded by the gene *norB*). All of the ammonia-oxidizing bacteria that have been screened to




date contain the *nirK* and *norB* genes (Casciotti and Ward, 2001; Shaw et al., 2006; Casciotti and Ward, 2005; Cantera and Stein, 2007; Norton et al., 2008; Arp et al., 2007), and members of several genera have demonstrated conversion of $^{15}NO_2^-$ to $^{15}N_2O$ (Poth and Focht, 1985; Shaw et al., 2006). Archaeal ammonia oxidizers also appear to possess *nirK* and *norB* homologs (Treusch et al., 2005; Hallam et al., 2006) but it is not known whether the proteins encoded by these genes are involved in $N_2O$ production.

The enzymes involved in nitrifier-denitrification are homologous to those found in a subset of heterotrophic denitrifying bacteria. However, unlike heterotrophic denitrification, nitrifier-denitrification may not be a strictly anaerobic process (Shaw et al., 2006). Ammonia-oxidizing bacteria express *nirK* in aerobic environments in response to $NO_2^-$ (Beaumont et al., 2004) and it has been hypothesized that NIR's main role is in detoxifying $NO_2^-$ (Poth and Focht, 1985; Beaumont et al., 2002). Nevertheless, a role for $O_2$ is suggested by the fact that *nirK* expression increases in low-$O_2$ conditions (Beaumont et al., 2004) and yields of $N_2O$ from cultures of ammonia-oxidizing bacteria increase by more than 40-fold when $O_2$ concentrations drop below 5 µM (Goreau et al., 1980).

$N_2O$ with biologically distinct origins can be identified using stable isotopic signatures. The oxygen isotopic signature ($\delta^{18}O–N_2O$) has been used to distinguish nitrification and denitrification $N_2O$ sources (Ostrom et al., 2000; Toyoda et al., 2005; Wrage et al., 2005; Kool et al., 2007). The $\delta^{18}O$ of $N_2O$ depends on the proportion of oxygen in $N_2O$ that is derived from $O_2$ versus $H_2O$, as well as any fractionation factors associated with incorporation or loss of the oxygen atoms in the metabolic precursors of $N_2O$ (Casciotti et al., 2010). $N_2O$ derived from $NH_2OH$ contains only oxygen atoms from $O_2$ whereas $N_2O$ produced by nitrifier-denitrification or heterotrophic denitrification depends on the $\delta^{18}O$ of $NO_2^-$ (and also $NO_3^-$ in the case of denitrification). $H_2O$ contributes a significant fraction of the oxygen in $NO_2^-$ and $NO_3^-$ during nitrification (Andersson et al., 1982; Casciotti et al., 2010; Buchwald and Casciotti, 2010). Since the $\delta^{18}O$ values of marine $H_2O$ are typically at least 20‰ less than those of dissolved $O_2$ (Kroopnick and Craig, 1976), marine $N_2O$ produced with different amounts of oxygen




from $H_2O$ and $O_2$ will reflect this in the $\delta^{18}O$ signature. Indeed, positive correlations between oceanographic $\delta^{18}O$-$O_2$ and $\delta^{18}O$-$N_2O$ data have been interpreted as evidence that the $N_2O$ is a product of nitrification because oxygen from $O_2$ is most directly incorporated into $N_2O$ through $NH_2OH$ during $NH_3$ oxidation (Ostrom et al., 2000; Andersson and Hooper, 1983).

However, there are potentially different isotope effects associated with the incorporation of oxygen atoms from $O_2$ and $H_2O$ into $N_2O$ (Casciotti et al., 2010). If these isotope effects are significant and variable among different species of ammonia oxidizers, it may prove difficult to extract source information based on oxygen isotopes alone. Furthermore, the $\delta^{18}O$ of $N_2O$ produced by ammonia-oxidizing bacteria may change depending on what fraction of the oxygen atoms are derived from $O_2$ (via $NH_2OH$ decomposition and nitrifier-denitrification) versus $H_2O$ (via nitrifier-denitrification).

The $\delta^{15}N$ site preference (SP) is another isotopic signature used to interpret environmental $N_2O$ data (Toyoda et al., 2002; Sutka et al., 2003, 2004; Toyoda et al., 2005; Sutka et al., 2006; Koba et al., 2009). SP as defined by Toyoda and Yoshida (1999) is the difference in the enrichment of the internal ($\alpha$) and external ($\beta$) nitrogen atoms in the linear $N_2O$ molecule:

$$SP = \delta^{15}N^{\alpha} - \delta^{15}N^{\beta}.$$

Unlike $\delta^{18}O$ and bulk $\delta^{15}N$ values, SP is thought to reflect the $N_2O$ production mechanism while remaining independent of the substrate's isotopic signature. This is because the reactions that produce $N_2O$ involve two identical precursor molecules (either NO or $NH_2OH$) (Toyoda et al., 2002; Schmidt et al., 2004) that are presumably drawn simultaneously from the same substrate pool. SP measurements made on $N_2O$ produced by ammonia-oxidizing bacteria and denitrifying bacteria support this idea (Sutka et al., 2006). Cultures of ammonia-oxidizing bacteria produce $N_2O$ with a SP of about 33.5‰ via $NH_2OH$ decomposition. However, in the presence of $NO_2^-$ or low $O_2$ concentrations, the same bacteria produce $N_2O$ with SPs that are closer to those of denitrifying bacteria (−0.8‰) (Sutka et al., 2003, 2004, 2006).



BGD
7, 3019–3059, 2010



Previous workers have estimated the "end-member" SP signatures of the two different sources of $N_2O$ in ammonia oxidizer cultures by manipulating $O_2$ concentrations in order to favor production via one process over the other. However, since $NH_2OH$ decomposition and nitrifier-denitrification can give rise to $N_2O$ simultaneously, failure to account for this mixing may cause errors in these end-member SP estimates. If $N_2O$ from $NH_2OH$ decomposition has a SP that is much higher than the SP of $N_2O$ from nitrifier-denitrification, as proposed by Sutka et al. (2003, 2004, 2006), then source mixing would cause underestimation of the SP of $NH_2OH$ decomposition and overestimation of the SP of nitrifier-denitrification.

Here we have used $\delta^{18}O$-$N_2O$ and SP measurements in combination with a biochemical model to make mixing-corrected estimates of the end-member SP values for $N_2O$ produced by $NH_2OH$ decomposition and nitrifier-denitrification by the marine ammonia-oxidizing bacterium *Nitrosomonas marina* C-113a. These end-member values were then used to calculate the $N_2O$ yields from nitrification and nitrifier-denitrification in different growth conditions, including a range of cell densities, $O_2$ concentrations (20%, 2%, and 0.5%), and $NO_2^-$ levels (0.2 to 1 mM), as well as in the presence of nitrite-oxidizing bacteria. Each experiment was carried out with an eye towards simulating environmental conditions more closely than previous studies by using growth medium that contains a fraction of the $NH_4^+$ present in commonly used recipes for ammonia oxidizer media (50 µM versus 5 to 10 mM $NH_4^+$).

## 2 Materials and methods

### 2.1 Culture maintenance and experimental setup

Cultures of *Nitrosomonas marina* C-113a were maintained in pure semi-continuous cultures with Watson medium containing 5 mM $NH_4^+$ (Watson, 1965). All maintenance cultures were kept in the dark at 25 °C with shaking at 100 rpm. The cultures used to inoculate experiments were periodically tested for heterotrophic contamination as fol-



BGD
7, 3019–3059, 2010



lows: 1 ml of each culture was added to 2 ml of a sterile 1:4 mixture of tryptic soy broth and artificial seawater and incubated 3 to 4 weeks in aerated culture tubes. Contamination was of particular concern during experiments on high density C-113a cultures because the abundance of cellular material was a potential source of organic substrate for the growth of heterotrophic denitrifiers, which can also produce $N_2O$ at low $O_2$ concentrations. For this reason, additional purity tests were done by inoculating 5 ml of each high density culture ($10^5 - 10^6$ cells $ml^{-1}$) into 10 ml of the sterile tryptic soy/artificial seawater mixture amended with 1 mM $NaNO2^-$). These cultures were incubated in closed, inverted 15 ml centrifuge tubes for 3 to 4 weeks. All tubes remained free of turbidity and showed no production of gas bubbles that would indicate heterotrophic denitrification.

Experiments were carried out in 545 ml glass serum bottles (Wheaton, 223952) that contained 100 ml sterile Watson medium with 50 µM $NH_4^+$. The headspace of each bottle was sealed using 30 mm gray butyl rubber septa (Wheaton, 224100-331) and aluminum crimps (Wheaton, 224187-01). Atmospheric $O_2$ and $N_2O$ were removed by purging for 3 h with $N_2$ flowing at $> 60$ ml $min^{-1}$ and appropriate amounts of high-purity $O_2$ ($\delta^{18}O$=+25.3‰) were injected back into each headspace to achieve 20%, 2%, or 0.5% $O_2$ ($v/v$) in the headspaces. Headspace $O_2$ and $N_2O$ concentrations were checked before and after each experiment (see below). The ratio of headspace to liquid volumes was such that complete $NH_3$ oxidation consumed less than 10% of the total $O_2$ in the lowest (0.5%) $O_2$ headspaces.

Immediately before each experiment, 1–2 l of late exponential or early stationary phase cultures were centrifuged at 10 000 g for 30 min, washed to remove residual $NH_4^+$ and $NO_2^-$, and re-suspended in 30 ml sterile media without $NH_4^+$. Experiments were initiated by the injection of 500 µl of washed and resuspended cells into each bottle. In the co-culture experiments, ammonia oxidizers with cell densities of approximately $2 \times 10^5$ cells $ml^{-1}$ were added with washed and resuspended cells of the nitrite-oxidizing bacterium *Nitrococcus mobilis* ($10^6$ cells $ml^{-1}$).

Initial and final cell densities were measured in samples preserved with 2% forma-



BGD
7, 3019–3059, 2010



lin (0.22-µm filtered) by making microscopic counts of DAPI-stained cells, or by using fluorescence assisted flow cytometry (FACS) to count SYBR green-stained cells on a FACS Calibur flow cytometer (Becton Dickinson). Uninoculated bottles served as a control for abiotic $N_2O$ production and were analyzed in parallel with experimental bottles. All bottles were incubated in the dark at room temperature with constant shaking. The progress of $NH_3$ oxidation was monitored by measuring accumulation of $NO_2^-$ and disappearance of $NH_4^+$ from the medium (see below). Once $NH_3$ oxidation was complete, experiments were terminated by injecting each bottle with 1 ml of 6 M NaOH, lysing the cells.

## 2.2 Chemical analyses

The concentrations of $NH_4^+$ were determined colorimetrically by the phenol-hypochlorite method (Solorzano, 1969) and $NO_2^-$ concentrations were determined by the Griess-Ilosvay colorimetric method (Pai and Yang, 1990) using a 1 cm path-length flow cell. Headspace $O_2$ concentrations were determined using a gas chromatograph with a $^{63}Ni$ electron capture detector (Shimadzu GC-8A). The $O_2$ peaks from 20 to 250 µl injections of sample headspace were recorded and integrated using Shimadzu EZStart software (v. 7.2.1). Sample peak areas were calibrated with standard injections of air. Headspace $N_2O$ concentrations were also measured before and after each experiment using the GC-8A. Sample peak areas were calibrated against commercial $N_2O$ mixtures (10, 1, and 0.1 ppm) and fresh atmospheric air (approximately 320 ppb). When total headspace $N_2O$ was less than 20 nmol, $N_2O$ was quantified by analyzing the whole bottle (by purging and trapping, see below) on a Finnigan Delta$^{PLUS}$ IRMS and using the linear relationship between peak area of *m/z* 44 and $N_2O$ mass to determine total $N_2O$. The average blank determined by analyzing bottles flushed with high-purity $N_2$ was 0.08±0.04 nmol.



BGD
7, 3019–3059, 2010



### 2.3 Isotopic analyses

Isotopic analyses of $N_2O$ were conducted using a Finnigan Delta$^{PLUS}$ XP isotope ratio mass spectrometer. Bottles were purged with He and $N_2O$ was cryo-trapped on-line with a custom-built purge and trap system (McIlvin and Casciotti, 2010) operated manually with 545 ml serum bottles. The following modifications made large volume gas extraction possible: bottles were loaded manually, the helium flow rate was increased to 60 ml min$^{-1}$, and the purge time was extended to 45 min. As described in McIlvin and Casciotti (2010), $CO_2$ was largely removed from the gas stream by passage through a Carbosorb trap, then $N_2O$ was separated from residual $CO_2$ using a capillary column (25 m×0.32 mm) lined with Poraplot-Q before injection into the mass spectrometer through an open split. Mass/charge (*m/z*) peak areas were automatically integrated using Isodat 2.0 software. Values for $\delta^{18}O$, $\delta^{15}N^{bulk}$, $\delta^{15}N^{\alpha}$, and $\delta^{15}N^{\beta}$ were obtained from simultaneous collection of the 45/44, 46/44, and 31/30 peak area ratios and referenced to our laboratory's $N_2O$ tank as described in Appendix A. This reference tank has been calibrated for $\delta^{18}O$ (‰ vs. VSMOW), $\delta^{15}N^{bulk}$, $\delta^{15}N^{\alpha}$, and $\delta^{15}N^{\beta}$ (‰ vs. AIR) by S. Toyoda (Tokyo Institute of Technology). Furthermore, the "scrambling coefficients" or isotopomer-specific $NO^+$ fragment ion yields for our Delta$^{PLUS}$ XP were determined for the ion source conditions used in these measurements (see Appendix B). For quality-control, two or three tropospheric $N_2O$ samples were analyzed between every 7 to 10 experimental samples to check the consistency of our isotopomer analyses. These samples were created by allowing 100 ml of artificial seawater to equilibrate with outside air in 545 mL serum bottles, sealing the bottles, and analyzing them as described above. Triplicate samples of tropospheric $N_2O$ from Woods Hole, MA analyzed during a typical run had $\delta^{15}N^{\alpha}$=15.0±0.1‰, $\delta^{15}N^{\beta}$=−1.9±0.1‰, $\delta^{18}O$=44.4±0.2‰, $\delta^{15}N^{bulk}$=6.5±0.1‰, SP=16.9±0.1‰, and *m/z* 44 peak area=15.6±0.2 mV-s.

We also measured the $\delta^{18}O$ and $\delta^{15}N$ of $NO_2^-$ that was produced by cultures as $NH_3$ oxidation progressed. $NO_2^-$ was converted to $N_2O$ using the azide method developed by McIlvin and Altabet (2005). The conversion to $N_2O$ was carried out immediately



BGD
7, 3019–3059, 2010



after sampling to avoid shifts in the oxygen isotopic values by abiotic exchange with water (Casciotti, 2007) or continued biological production of $NO_2^-$ from residual $NH_3$. Individual sample volumes were adjusted so that a consistent amount of $N_2O$ (5 or 10 nmol) was produced for each set of azide reactions. Each sample set included at least three sets of three different $NO_2^-$ standards (N-23, N-7373, and N-10219, Casciotti, 2007) that were used to calculate sample $\delta^{15}N$ (‰ vs. AIR) and $\delta^{18}O$ (‰ vs. VSMOW) values. These samples were analyzed in 20 ml headspace vials using the autosampler setup described by Casciotti et al. (2002), modified with the addition of an −60° C ethanol trap and column backflush (McIlvin and Casciotti, 2010).

## 3 Results and discussion

Nitrifier-denitrification depends on the presence of $NO_2^-$ to produce $N_2O$ (Ritchie and Nicholas, 1972; Poth and Focht, 1985; Yoshida, 1988), and the accumulation of $NO_2^-$ in environments such as oxygen deficient zones (ODZs) could contribute to increased $N_2O$ production in these regions. This study was designed to test the impact of $O_2$ and $NO_2^-$ concentrations on the $N_2O$ yield of marine ammonia-oxidizing bacteria at a lower substrate ($NH_4^+$) concentration, and at a broader and lower range of cell densities than any previous work. To date, the roles of substrate concentration and cell density in determining $N_2O$ yield have not been resolved. $N_2O$ yield data are presented in the same form used in oceanographic $N_2O$ studies so that yields refer to the fraction of N atoms converted to $N_2O$ out of the total amount of $NH_3$ that is oxidized (i.e. 2×moles $N_2O$/moles $NH_3$). In other words, a yield of $5\times10^{-4}$ indicates that 1 in every 2000 N atoms from oxidized $NH_3$ will go into an $N_2O$ molecule.

### 3.1 Cell density and $O_2$ concentration

Cell density influenced the observed $N_2O$ yields in both low $O_2$ (0.5% and 2%) and high $O_2$ (20%) conditions. $O_2$ concentration had the greatest impact on $N_2O$ yield at

the highest starting cell density tested ($1.5\times10^6$ cells $ml^{-1}$) (Fig. 1). At 20% $O_2$, the high density cultures had the lowest yields, on average $1.3\pm0.4\times10^{-4}$, while at 0.5% $O_2$ the high density cultures had the highest average yields observed, $220\pm40\times10^{-4}$. In contrast, $O_2$ had a much smaller impact on $N_2O$ yield in the medium density cultures (starting density of $2.1\times10^4$ cells $ml^{-1}$) and the low density cultures (starting density=$2\times10^2$ cells $ml^{-1}$). In fact, the $N_2O$ yields of the medium density cultures were not significantly different among the high and low $O_2$ treatments ($5.1\pm0.5\times10^{-4}$ at 20% $O_2$, $5.5\pm0.8\times10^{-4}$ at 2% $O_2$, $6.4\pm1.4\times10^{-4}$ at 0.5% $O_2$). Low density cultures produced average yields of $3.9\pm0.3\times10^{-4}$ at 20% $O_2$, $4.7\pm0.1\times10^{-4}$ at 2% $O_2$, and $6.7\pm0.5\times10^{-4}$ at 0.5% $O_2$.

The average yields of the cultures at 20% $O_2$ ($1.3–5\times10^{-4}$) were comparable to the production yields ($0.8–5.4\times10^{-4}$) measured by Yoshida et al. (1989) in the oxic surface waters of the western North Pacific using $^{15}NH_4^+$ tracer techniques. However, they are lower than previously reported yields for *Nitrosomonas* cultures at 20% $O_2$ ($26–30\times10^{-4}$ in Goreau et al. (1980) and $10–390\times10^{-4}$ in Remde and Conrad, 1990).

In this study, low-$O_2$ conditions only resulted in substantial increases in $N_2O$ yield when cell densities were artificially high. $N_2O$ yields were relatively low and less sensitive to $O_2$ when cell densities were close to those observed in the ocean ($10^3–10^4$ cells $l^{-1}$, Ward et al., 1982). This draws into question the oceanographic applicability of previous culture-based yield measurements, where a many-fold increase in $N_2O$ yield was observed as $O_2$ dropped from 20% to 0.5% (Goreau et al., 1980). Goreau et al. (1980) worked with a marine *Nitrosomonas* strain at cell densities ($1\times10^6$ cells $ml^{-1}$) comparable to our high density experiments and observed $N_2O$ yields of $800–1000\times10^{-4}$ for cultures grown at 0.5% $O_2$. The implication of the present study is that other factors (such as cell density) influence the relationship between $N_2O$ yield and $O_2$ concentration.

The mechanisms that explain the high $N_2O$ yields of high density cultures at low $O_2$ could be chemical or biological. $O_2$ has a major influence on the half-life of nitric



BGD
7, 3019–3059, 2010



oxide (NO), the gaseous precursor of $N_2O$ during nitrifier-denitrification. Concentration-dependent changes in the rate of $N_2O$-production could be related to $O_2$ as a consequence of the abiotic oxidation of NO:

$$2NO + O_2 \rightarrow 2NO_2$$

$$2NO_2 + H_2O \rightarrow HNO_2 + HNO_3,$$ Ritchie and Nicholas (1972),

where nitrous acid ($HNO_2$), is the major decomposition product of the second reaction (Ignarro et al., 1993). In oxygenated environments, $O_2$ is the major reactant so that the reaction obeys pseudo-first-order kinetics (Lewis and Deen, 1994). However, in low-$O_2$ environments the half-life of NO increases, so that during bacterial $NH_3$ oxidation, it can accumulate to concentrations that are similar to $N_2O$ (Remde and Conrad, 1990; Lipschultz et al., 1981). This may allow enzymatic NO reduction to $N_2O$ during nitrifier-denitrification to compete for NO with the above $O_2$-dependent reaction. Studies of *N. europaea* have also shown that the expression of *nirK* during nitrifier-denitrification is controlled by a repressor protein that belongs to a family of NO-sensitive transcription regulators (Rodionov et al., 2005; Beaumont et al., 2002, 2004). If NO induces *nirK* transcription, the abiotic reaction of $O_2$ with NO could impact NIR-dependent $N_2O$ production by destroying the gene's inducer, NO. High cell densities may be necessary for either of these effects to take hold because biological competition with $O_2$ for NO will depend on the diffusivities of $O_2$ and NO relative to the distance between cells.

It is unclear why the highest density cultures had significantly lower $N_2O$ yields at 20% $O_2$ than cultures with lower cell densities (Fig. 1), but it may be related to the amount of time that it took each culture to oxidize all of the $NH_4^+$ present. The medium- and low-density cultures took 3.5 and 14 days to oxidize 50 µM $NH_4^+$, respectively, while the high density cultures took 7 h. The bacteria in the medium- and low-density cultures may have had time to adjust their gene expression and enzyme activity to experimental conditions, whereas the high-density cultures did not. The discrepancy could also be related to differences in cell growth and division. Cell numbers doubled approximately 7, 2, and 0 times, in the low-, medium-, and high-density cultures, respectively. Rapidly

growing cells may be less efficient at converting $NH_2OH$ to $NO_2^-$, allowing more $NH_2OH$ to decompose into $N_2O$.

### 3.2 $NO_2^-$ and $O_2$ concentration

$NO_2^-$ concentrations are sub-micromolar throughout most of the ocean. Yet in pure batch cultures of ammonia oxidizers, $NO_2^-$ exposure is an unavoidable result of growth because $NO_2^-$ increases up to the initial $NH_4^+$ concentration. Excess $NO_2^-$ may increase $N_2O$ yields if ammonia oxidizers convert $NO_2^-$ to $N_2O$ to avoid the toxic effects of $NO_2^-$ (Poth and Focht, 1985; Beaumont et al., 2002, 2004). Our experiments contained lower $NH_4^+$ concentrations and therefore lower amounts of $NO_2^-$ than previous studies. To test the impact of $NO_2^-$ on $N_2O$ yields, we increased $NO_2^-$ concentrations by adding 0.2 or 1 mM $NO_2^-$ to some cultures, and decreased accumulated $NO_2^-$ concentrations in others by adding the nitrite-oxidizing bacterium *Nitrococcus mobilis* to create a co-culture.

The addition of 1 mM $NO_2^-$ had a greater impact on $N_2O$ yield than differences in $O_2$ concentration (Fig. 2a). The increase due to the additional $NO_2^-$ was apparent in both low and high $O_2$ conditions. Furthermore, the average $N_2O$ yields increased as the amount of added $NO_2^-$ increased. Cultures under 20% $O_2$ with no added $NO_2^-$ had an average yield of $4.0\pm0.03\times10^{-4}$ while those with 1 mM added $NO_2^-$ had an average yield of $7.6\pm0.5\times10^{-4}$. Cultures under 0.5% $O_2$ with no added $NO_2^-$ had an average yield of $6.0\pm0.5\times10^{-4}$ and those with 1 mM added $NO_2^-$ had an average yield of $10.2\pm0.3\times10^{-4}$. $N_2O$ yields were calculated as a fraction of the total N in $NH_4^+$ at the start of the experiment ($5\times10^{-6}$ moles). There was no detectable loss of dissolved N from the combined $NH_4^+$ and $NO_2^-$ pools.

In the co-cultures, $NO_2^-$ concentrations remained below detection at 20% $O_2$ and below 17 µM at 0.5% $O_2$. Although co-culturing kept $NO_2^-$ concentrations lower than they were in the pure cultures, $N_2O$ yields were not significantly lower in the presence of the nitrite-oxidizing bacteria (Fig. 2b). The insignificant differences between the



BGD
7, 3019–3059, 2010



yields with and without nitrite oxidizers suggests that the 50 µM $NO_2^-$ that accumulated in our pure cultures did not have a major impact on the $N_2O$ yields measured for those cultures. However, we were unable to entirely eliminate $NO_2^-$ accumulation in the low-$O_2$ experiments. Future work should focus on identifying the impact of $NO_2^-$ on $N_2O$ production by nitrifiers in low-$O_2$ environments.

The role of $NO_2^-$ in the biochemistry of ammonia oxidizers can be both stimulatory and inhibitory. *N. europaea* cultures that have been starved for $NH_3$ demonstrate increased potential $NH_3$ oxidizing activity in the presence of 5 mM $NO_2^-$ (Laanbroek et al., 2002), indicating that $NO_2^-$ has protective properties. On the other hand, the same species exhibits reduced growth in the presence of higher $NO_2^-$ concentrations (10–100 mM) (Beaumont et al., 2004). Environmentally-relevant ammonia oxidizers may also have lower $NO_2^-$ tolerances than laboratory strains like *N. europaea* that are regularly exposed to high $NO_2^-$ concentrations. The relationship between $NO_2^-$, nitrifier-denitrification, and $N_2O$ production is also complex. Aerobic *nirK* expression occurs in response to increasing $NO_2^-$ concentrations (Beaumont et al., 2004), but *nirK* knock-out mutants actually produce more $N_2O$ than the wild-type strain (Beaumont et al., 2002).

Oceanic $O_2$ concentrations may influence a number of different biogeochemical variables that enhance $N_2O$ production by ammonia oxidizers. For example, low $O_2$ concentrations can increase the biological turnover time of $NO_2^-$ (Hashimoto et al., 1983) because the activity of nitrite-oxidizing bacteria ceases at a higher $O_2$ concentration than the activity of ammonia-oxidizing bacteria (Helder and de Vries, 1983). Charpentier et al. (2007) also suggest that high concentrations of organic particles found in certain productive waters enhance $N_2O$ production by creating high-$NO_2^-$, low-$O_2$ microenvironments necessary to support nitrifier-denitrification. Future oceanographic work should investigate how $N_2O$ production rates in oxygen deficient zones (ODZs) relate to these different biogeochemical variables.

### 3.3 Pathway dependence of $\delta^{15}N^{bulk}$-$N_2O$

The bulk $\delta^{15}N$ of biological $N_2O$ ($\delta^{15}N^{bulk}$-$N_2O$) depends on the $\delta^{15}N$ of the substrate and any kinetic isotope effects associated with the enzymes that produce the $N_2O$. Cultures of ammonia-oxidizing bacteria produce $N_2O$ that is generally depleted in $^{15}N$ relative to the substrate $NH_3$ or the $NO_2^-$ produced (Yoshida, 1988; Sutka et al., 2003, 2004, 2006). This observation has been used to argue against nitrification as the source of $N_2O$ in waters such as the western North Pacific, where $N_2O$ is actually more enriched in $^{15}N$ than the ambient $NO_3^-$ (Yoshida et al., 1989). However, the $\delta^{15}N$ of other $N_2O$ precursors like $NH_2OH$ (or $NH_3$) and $NO_2^-$ are difficult to measure because their oceanic concentrations are generally quite low.

Ammonia-oxidizing bacteria make $N_2O$ through two different pathways, so that the observed isotopic signatures of $N_2O$ are a function of the pathways' mixing fractions, the isotopic signatures of their different substrate molecules, and the different isotope effects associated with those pathways. To probe the range of $N_2O$ isotopic signatures made by C-113a, we manipulated growth conditions such as $O_2$ concentration and cell density in order to favor one $N_2O$ production mechanism over another during complete oxidation of 5 µmoles of $NH_3$ (Figs. 3 and 4). We have interpreted the observed variation in $\delta^{15}N^{bulk}$-$N_2O$ to account for pathway-dependent mixing with different isotope effects and $\delta^{15}N$ signatures for $N_2O$ produced through the different pathways. The goal in separating out the isotopic characteristics of the two processes was to determine the full range of $N_2O$ isotopic signatures that can be produced by this ammonia oxidizer. We note that it was impossible to decouple nitrifier-denitrification from the $NH_2OH$ decomposition pathway by growing C-113a in the presence of $NO_2^-$ alone because the bacteria do not produce $N_2O$ unless there is also $NH_4^+$ present in the media (unpublished observations).

$N_2O$ produced by all C-113a cultures was depleted in $^{15}N$ relative to the substrate $NH_3$ ($\delta^{15}N$-$NH_4^+$ = −3‰), although the range varied widely ($\delta^{15}N^{bulk}$-$N_2O$ = −54.9‰ to

−6.6‰, Fig. 3). Culture conditions affected the degree of $^{15}N$ depletion, with cultures grown under 0.5% $O_2$ producing the most depleted $N_2O$ (−54.9‰ to −15.2‰), while cultures grown with 20% $O_2$ generally produced $N_2O$ with higher $\delta^{15}N$ values (−13.6‰ to −6.7‰). The low-$O_2$ cultures that produced the most depleted $N_2O$ also produced the most $N_2O$ (highest yield). We interpret the results by assuming each datapoint ($\delta^{15}N^{bulk}_{total}$, $M_{total}$) represents a two-component mixture of a constant or "basal" $N_2O$ source from $NH_2OH$ decomposition ($M_{NH_2OH}$) and a variable source of $N_2O$ from nitrifier-denitrification ($M_{ND}$) that tended to be larger in low-$O_2$ cultures. This is the basis for performing the type II linear regression of $\delta^{15}N^{bulk}$ versus $\frac{1}{\text{mass } N_2O}$ in Fig. 3. Equation (3b) (below), the model for the linear regression, was developed using the mass balance Eqs. (1) and (2):

$$\delta^{15}N^{bulk}_{total} \times M_{total} = \delta^{15}N^{bulk}_{ND} \times M_{ND} + \delta^{15}N^{bulk}_{NH_2OH} \times M_{NH_2OH} \quad (1)$$

$$M_{ND} = M_{total} - M_{NH_2OH} \quad (2)$$

$$\delta^{15}N^{bulk}_{total} = \frac{\delta^{15}N^{bulk}_{ND} \times (M_{total} - M_{NH_2OH}) + \delta^{15}N^{bulk}_{NH_2OH} \times M_{NH_2OH}}{M_{total}} \quad (3a)$$

$$\delta^{15}N^{bulk}_{total} = (\delta^{15}N^{bulk}_{NH_2OH} \times M_{NH_2OH} - \delta^{15}N^{bulk}_{ND} \times M_{NH_2OH}) \times \frac{1}{M_{total}} + \delta^{15}N^{bulk}_{ND} \quad (3b)$$

According to Eq. (3b), the y-intercept of the regression is the $\delta^{15}N^{bulk}$ of the more depleted nitrifier-denitrification end-member ($\delta^{15}N^{bulk}_{ND}$). The value of $\delta^{15}N^{bulk}_{ND}$ obtained in this way is −60.6‰±4.1‰ (errors are given as one standard deviation of the y-intercept). The difference between the $\delta^{15}N^{bulk}$ of the product $N_2O$ and the $\delta^{15}N$ of the starting $NH_3$ is the overall isotope effect associated with $N_2O$ formation by nitrifier denitrification ($^{15}\epsilon_{ND}$=−57.6‰). The most enriched $N_2O$ produced in these experiments had a $\delta^{15}N^{bulk}$ of −6.7‰, providing a minimum $\delta^{15}N^{bulk}$ for $M_{NH_2OH}$ (since a mixture



BGD
7, 3019–3059, 2010



of $N_2O$ that has one −60.6‰ end-member must also have a heavier end-member in order to produce an $N_2O$ mixture with an intermediate $\delta^{15}N^{bulk}$).

This end-member mixing model does not account for the Rayleigh effects that kinetic isotopic fractionation has in closed systems such as batch cultures. These effects change the isotopic signatures of the $NH_3$ that is consumed and the $NO_2^-$ that accumulates as $NH_3$ oxidation proceeds (Mariotti et al., 1981) so that at any instant during the reaction, the $\delta^{15}N$ of $N_2O$ produced from these substrates will also reflect these isotopic shifts. However in this study, the end-member mixing model is not a serious violation of Rayleigh assumptions because all cultures were allowed to oxidize the same amount of $NH_3$ to completion before the total $N_2O$ was analyzed. Abrupt changes in $N_2O$ production rates during the $NH_3$ oxidation reaction could also make this model problematic in a Rayleigh system. However, in these experiments $N_2O$ accumulated steadily as $NH_3$ oxidation progressed and $NO_2^-$ accumulated (Fig. S1, see supplemetary material http://www.biogeosciences-discuss.net/7/3019/2010/bgd-7-3019-2010-supplement.zip).

### 3.4 Covariation of SP and $\delta^{18}O$-$N_2O$

The $\delta^{18}O$ of $N_2O$ is like $\delta^{15}N^{bulk}$ in that these signatures are both pathway-dependent and substrate-dependent. That is, the $\delta^{18}O$ of $N_2O$ produced by ammonia-oxidizing bacteria depends on the mixing fraction of the two $N_2O$ pathways as well as the isotopic signatures of the substrates ($O_2$ and $H_2O$) that contribute oxygen atoms to those pathways and isotopic fractionation during oxygen atom incorporation or loss in the reactions that produce $N_2O$ (Casciotti et al., 2010). The conversion of $NH_3$ to $NO_2^-$ incorporates oxygen atoms from $O_2$ and $H_2O$ (Andersson et al., 1982; Andersson and Hooper, 1983):

$$NH_3 + \frac{1}{2}O_2 \rightarrow NH_2OH$$

$$NH_2OH + H_2O \rightarrow HNO_2 + 4H\cdot$$



BGD
7, 3019–3059, 2010



We expect the $\delta^{18}O$ of $N_2O$ derived from $NH_2OH$ decomposition to be independent of the $\delta^{18}O$ of $H_2O$ because $O_2$ is the sole contributor of oxygen during the first reaction. However, the $\delta^{18}O$ of $N_2O$ produced by $NO_2^-$ reduction during nitrifier-denitrification depends upon both the $\delta^{18}O$-$O_2$ and $\delta^{18}O$-$H_2O$, in proportions that are affected by the amount of oxygen atom exchange between $NO_2^-$ and $H_2O$ (Andersson and Hooper, 1983; Casciotti et al., 2002; Kool et al., 2007; Casciotti et al., 2010).

The fact that the $\delta^{18}O$ of $N_2O$ produced by nitrifier-denitrification is sensitive to changes in $\delta^{18}O$-$H_2O$ is the basis for a technique that uses parallel experiments in $^{18}O$-labeled and unlabeled $H_2O$ to identify the proportion of $N_2O$ produced by nitrifier-denitrification (Wrage et al., 2005). The difference in $\delta^{18}O$ of $N_2O$ from ammonia oxidizers grown in labeled and unlabeled $H_2O$ is directly proportional to the fraction of the total $N_2O$ that is produced by nitrifier-denitrification. Note that in these experiments, side-by-side comparisons between labeled and unlabeled replicates assume that nitrifier-denitrification and $NH_2OH$ decomposition contribute the same proportion of $N_2O$ to both labeled and unlabeled replicates and that the $N_2O$ from $NH_2OH$ decomposition has the same $^{18}O$ signature in both labeled and unlabeled experiments.

The impact of $\delta^{18}O$-$H_2O$ on the $\delta^{18}O$ of $N_2O$ produced by C-113a is demonstrated in Fig. 4, where cultures grown in water with a $\delta^{18}O$ of +40‰ produced $N_2O$ that was 5‰ to 40‰ more enriched in $^{18}O$ than cultures grown in $H_2O$ with a $\delta^{18}O$ of −5‰. The difference between labeled and unlabeled cultures was greatest at 0.5% $O_2$, whereas at higher $O_2$ concentrations, the $\delta^{18}O$-$N_2O$ values converged. The pattern is consistent with larger $N_2O$ contributions by nitrifier-denitrification as $O_2$ concentrations drop and $H_2O$ contributes more to the overall $\delta^{18}O$-$N_2O$.

In contrast to $\delta^{18}O$-$N_2O$, SP signatures of $N_2O$ from ammonia oxidizers are thought to be pathway-dependent and substrate-independent: SP signatures vary as a result of mixing among $N_2O$ sources with distinct SP values (Sutka et al., 2003, 2004, 2006), but they do not depend on the $\delta^{15}N$ values of the $N_2O$ precursor molecules (Toyoda et al., 2002). For example, *N. europaea* produces high-SP $N_2O$ (31.4±4.2‰) when



BGD
7, 3019–3059, 2010



growing aerobically on $NH_3$, presumably through $NH_2OH$ decomposition (Sutka et al., 2006). However, it can also produce low-SP $N_2O$ ($-0.8\pm5.8$‰) in the presence of $NO_2^-$ and anaerobic conditions during nitrifier-denitrification (Sutka et al., 2003, 2004). In the present study, C-113a also produced high-SP $N_2O$ (up to 33.2‰) under 20% $O_2$ and low-SP $N_2O$ (down to −9.1‰) under 0.5% $O_2$ (Fig. 4).

Knowing the end-member SP signatures of $N_2O$ from $NH_2OH$ decomposition and nitrifier-denitrification is powerful because these can then be used to calculate the size of each pathway's contribution to a culture's total $N_2O$ output based on its SP signature ($SP_{total}$) (Charpentier et al., 2007). We used the following model to extract these end-member SP signatures from our culture data, accounting for the fact that the SP of the $N_2O$ from each culture is a mixture of these end-members. Following Charpentier et al. (2007), we set up a system of isotopic mass balance equations that describe isotopic mixing between low-SP $N_2O$ from nitrifier-denitrification ($SP_{ND}$) and high-SP $N_2O$ from $NH_2OH$ decomposition ($SP_{NH_2OH}$):

$$SP_{total} = F_{ND} \times SP_{ND} + (1 - F_{ND}) \times SP_{NH_2OH}, \quad (4a)$$

where $F_{ND}$ is the fraction of total $N_2O$ that is produced by nitrifier-denitrification. Solving Eq. (4a) for $F_{ND}$ produces:

$$F_{ND} = \frac{SP_{total} - SP_{NH_2OH}}{SP_{ND} - SP_{NH_2OH}} \quad (4b)$$

Equation (4b) cannot be solved for $F_{ND}$ without knowing the end-member values, $SP_{ND}$ and $SP_{NH_2OH}$, or having additional information about the value of $F_{ND}$ for each data point. Therefore, we develop a complementary mixing equation based on the $\delta^{18}O$-$N_2O$:

$$\delta^{18}O\text{-}N_2O_{total} = F_{ND} \times (\delta^{18}O\text{-}NO_2^- + {}^{18}\varepsilon_{ND}) + (1 - F_{ND}) \times (\delta^{18}O\text{-}O_2 + {}^{18}\varepsilon_{NH_2OH}) \quad (5)$$

As discussed above, the measured $\delta^{18}O$-$N_2O$ ($\delta^{18}O$-$N_2O_{total}$) depends not only on the mixing fraction $F_{ND}$, but also the isotopic signatures of the substrate molecules

($\delta^{18}$O-$NO_2^-$ and $\delta^{18}$O-$O_2$) and kinetic and/or branching isotope effects associated with either reaction ($^{18}\epsilon_{NH_2OH}$ and $^{18}\epsilon_{ND}$). In these equations, $^{18}\epsilon_{NH_2OH}$ and $^{18}\epsilon_{ND}$ are the net isotope effects expressed during oxygen incorporation from either $O_2$ or $NO_2^-$ into $N_2O$. Here we do not consider the impact of Rayleigh fractionation on the $\delta^{18}$O-$O_2$ because the $O_2$ pool is large relative to the fraction that is consumed (<10%) and is expected to raise the $\delta^{18}$O-$O_2$ less than 2‰. Substituting Eq. (4b) into (5) produces Eq. (6), which includes both SP values and oxygen isotopic signatures:

$$\delta^{18}O\text{-}N_2O_{total} = \frac{SP_{total} - SP_{NH_2OH}}{SP_{ND} - SP_{NH_2OH}} \times (\delta^{18}O\text{-}NO_2^- - \epsilon_{ND}) + \left(1 - \frac{SP_{total} - SP_{NH_2OH}}{SP_{ND} - SP_{NH2OH}}\right) \times \left(\delta^{18}O\text{-}O_2 - \epsilon_{NH_2OH}\right) \quad (6)$$

The best-fit values of the parameters $SP_{NH_2OH}$, $SP_{ND}$, $\epsilon_{NH_2OH}$, and $\epsilon_{ND}$ (Table 1) were obtained by fitting Eq. (6) to our dataset ($n = 32$) using a Levenberg-Marquardt non-linear regression program (Draper and Smith, 1981). Inputs were the values of $SP_{total}$, $\delta^{18}$O-$N_2O$, and $\delta^{18}$O-$NO_2^-$ measured for each culture, as well as the known $\delta^{18}$O of the high-purity $O_2$ used in the headspaces (+25.3‰). Our estimates of the end-member SP values of $N_2O$ are significantly lower (−10.7±2.9‰) for $N_2O$ produced by nitrifier-denitrification and higher (36.3±2.4‰) for $N_2O$ produced by $NH_2OH$ decomposition than previous estimates (Sutka et al., 2003, 2004, 2006).

These results expand the range of SP values produced by ammonia oxidizers by more than 10‰. This has an impact when Eq. (4b) is used to calculate the fraction of $N_2O$ from nitrifier-denitrification using oceanographic SP data (Charpentier et al., 2007). Here we used the new end-member SP values to calculate that nitrifier-denitrification by C-113a accounted for 11% to 26% of $N_2O$ production under 20% $O_2$ and 43% to 87% of production under 0.5% $O_2$ (Table 2). There was considerable variation among cultures with different cell densities, with denser cultures producing relatively more $N_2O$ by nitrifier-denitrification at low-$O_2$ and less at high-$O_2$.



BGD
7, 3019–3059, 2010



A sensitivity analysis on the model reveals that estimates of $SP_{NH_2OH}$ and $SP_{ND}$ are both very sensitive to the values of the isotope effects $\epsilon_{NH_2OH}$ and $\epsilon_{ND}$, although the sensitivity to $\epsilon_{NH_2OH}$ decreases in labeled $H_2O$ (Fig. S2a–d, see http://www.biogeosciences-discuss.net/7/3019/2010/bgd-7-3019-2010-supplement.pdf). There are few published estimates of these isotope effects that we can compare with our model results, although recent work has addressed the isotope effects for oxygen atom incorporation into $NH_2OH$ and $NO_2^-$ by C-113a (Casciotti et al., 2010). Work on the heterotrophic denitrifier *Pseudomonas aureofaciens* indicates that the branching oxygen isotope effect of $NO_2^-$ reduction is approximately 25‰ (Casciotti, 2007). However, it is not known whether the same isotope effect applies to nitrifier-denitrification or if there is also a kinetic isotope effect that influences the $\delta^{18}O$ of $N_2O$.

Equation (6) assumes that the oxygen atoms in $N_2O$ produced by $NH_2OH$ decomposition come only from $O_2$. If a fraction of this oxygen actually comes from $H_2O$ then the model value of $\epsilon_{NH_2OH}$ should be too low for data from experiments in unlabeled $H_2O$ ($\delta^{18}O$-$H_2O$<$\delta^{18}O$-$O_2$) and too high for data from labeled $H_2O$ ($\delta^{18}O$-$H_2O$>$\delta^{18}O$-$O_2$). However, this pattern was not apparent in the residuals of $\epsilon_{NH_2OH}$ from labeled versus unlabeled experiments. Furthermore, if oxygen atoms exchanged between $H_2O$ and $NH_2OH$ is occurring, there was too much scatter in the data to resolve it by including an exchange term in Eq. (6).

The $\delta^{18}O$ and SP signatures of the $N_2O$ in these experiments covaried (Fig. 4). The covariation depended on the $\delta^{18}O$ of the $H_2O$ in the media: the slope of the linear regression of SP and $\delta^{18}O$-$N_2O$ was negative (−0.904±0.087) for experiments performed in $^{18}O$-enriched $H_2O$ (40‰) and positive (0.152±0.044) for experiments in $^{18}O$-depleted $H_2O$ (−5‰) (Fig. 4). Our model provides an explanation for the covariation between SP and $\delta^{18}O$-$N_2O$ because it describes mixing between two $N_2O$ sources with distinct SP values and different proportions of oxygen from $O_2$ and $H_2O$. According to Eq. (6), the sign and magnitude of the regression slope will depend upon the difference between $\delta^{18}O$-$O_2$ and $\delta^{18}O$-$H_2O$.



BGD
7, 3019–3059, 2010



Positive correlations between $\delta^{18}$O-$N_2O$ and SP observed in environmental data have been interpreted as signs that $N_2O$ consumption by denitrification is an important $N_2O$ cycling process in the system under scrutiny (Koba et al., 2009; Yoshida and Toyoda, 2000; Popp et al., 2002; Toyoda et al., 2002; Schmidt et al., 2004). Indeed, there is experimental evidence demonstrating that progressive consumption of $N_2O$ by denitrifier cultures results in a simultaneous increase in both SP and $\delta^{18}$O-$N_2O$ (Ostrom et al., 2007). The theoretical basis for this behavior is the fact that the N-O bonds formed by the heavier nitrogen and oxygen isotopes have lower zero-point energies and are therefore more resistant to being broken than bonds between the lighter isotopes (Yung and Miller, 1997; Toyoda et al., 2002). As a result, decomposition of a symmetrical O-N-N-O intermediate during $N_2O$ formation and also cleavage of the N-O bond during $N_2O$ reduction to $N_2$ will produce $N_2O$ with positively correlated $\delta^{18}$O and SP values.

Our work demonstrates that SP and $\delta^{18}$O-$N_2O$ can also covary as a result of $N_2O$ production by nitrification, without the need to invoke $N_2O$ consumption by heterotrophic denitrifiers. The sign and magnitude of the correlation depends on the difference between the $\delta^{18}$O of the $O_2$ and the $H_2O$ that contribute oxygen atoms to the $N_2O$. In contrast to this study, where we manipulated $\delta^{18}$O-$H_2O$, there is little natural variation in $\delta^{18}$O-$H_2O$ in the open ocean but much larger variation in $\delta^{18}$O-$O_2$ as a result of isotopic fractionation associated with respiratory $O_2$ consumption (Kroopnick and Craig, 1976; Bender, 1990; Levine et al., 2009). According to model Eq. (6), we would expect the slopes of the $\delta^{18}$O-SP regressions (such as those in Fig. 4) to increase as $\delta^{18}$O-$O_2$ rises relative to $\delta^{18}$O-$H_2O$ (or $\delta^{18}$O-$NO_2^-$). $N_2O$ from nitrification may therefore influence the dynamics between $\delta^{18}$O-$N_2O$ and SP in the oxycline in two opposing ways : 1) a drop in $O_2$ concentration may promote nitrifier-denitrification and thus the incorporation of low-$\delta^{18}$O oxygen atoms from $H_2O$ into low-SP $N_2O$ and 2) respiratory $O_2$ consumption increases the $\delta^{18}$O of the remaining $O_2$ pool, raising the $\delta^{18}$O of the $N_2O$ produced by $NH_2OH$ decomposition as well as nitrifier-denitrification.



BGD
7, 3019–3059, 2010



In the future, the combined measurement of SP, $\delta^{18}$O-$N_2O$, and $\delta^{18}$O-$O_2$ may be used to resolve these effects.

## 4 Conclusions

As shown previously, culturing conditions influence $N_2O$ yields from ammonia-oxidizing bacteria. However, yields observed in this study were much lower than those obtained in previous culture-based measurements, and they did not increase as dramatically at low oxygen tensions. These results are in line with modeling- and incubation-based oceanographic estimates of $N_2O$ yields from nitrification and may be useful in future modeling of $N_2O$ production and distributions in the ocean. Recent work interpreting isotopic signatures of biogenic $N_2O$ has often relied on the assumption that a direct relationship between $\delta^{18}$O-$N_2O$ and SP was indicative of $N_2O$ consumption and production by denitrification. However, our work suggests that a direct relationship between these signatures may also occur as a result of nitrification, at least when the SP values vary between −10‰ and 36‰. Nitrification produces this relationship through mixing between high-SP, $^{18}$O-enriched $N_2O$ produced by $NH_2OH$ decomposition and low-SP, $^{18}$O-depleted $N_2O$ produced by nitrifier-denitrification. When interpreting the marine $N_2O$ cycle using isotopic signatures, a major unknown is whether archaeal ammonia oxidizers also produce $N_2O$ and if so, what their impact is on the $N_2O$ budget and the isotopic signatures of $N_2O$ in the ocean. The genome of *Cenarchaeum symbiosum* contains genes that are homologous to bacterial *nirK* but not for hydroxylamine oxidoreductase (Hallam et al., 2006). If the archaeal system of converting $NH_3$ to $NO_2^-$ is profoundly different from the bacterial one, it could influence how $O_2$ is incorporated into $NO_2^-$ and thus the value of $\delta^{18}$O-$N_2O$, as well as SP and $\delta^{15}N^{bulk}$-$N_2O$.





## Appendix A

Data collected during continuous flow isotopic analyses of $N_2O$ included simultaneous signal intensities (in volt-seconds) of mass/charge (*m/z*) detectors 30, 31, 44, 45, and 46. The delta values and site preferences reported here were calculated using the raw peak area ratios of 31/30, 45/44, and 46/44 for a reference gas injection and the eluted sample peak. Isodat reports these raw ratios as "rR 31NO/30NO", etc. For each run, sample raw ratios were referenced to the standard ratios, and these ratio ratios were multiplied by the appropriate standard ratios ($^{31}R_{standard}$=0.004054063, $^{45}R_{standard}$=0.007743032, $^{46}R_{standard}$=0.002103490) to calculate $^{31}R_{sample}$, $^{45}R_{sample}$, and $^{46}R_{sample}$, respectively. For example, $^{31}R_{sample}$=[(rR 31NO/30NO)$_{sample}$]/[(rR 31NO/30NO$_{standard}$)]·$^{31}R_{standard}$.

The $R_{standard}$ values are the calculated ratios that the Farraday cups in the Casciotti MS should detect whenever the standard gas is analyzed under normal operating conditions. They depend on the actual isotopic/isotopomeric composition of the standard gas and also how that gas is fragmented in the MS. To calculate these three values we used 1) values of $\delta^{15}N^{\alpha}$, $\delta^{15}N^{\beta}$, and $\delta^{18}O$ for our standard gas as measured by Sakae Toyoda and 2) The relative yields of *m/z* 30 and 31 from the $^{15}N^{14}NO$ and $^{14}N^{15}NO$ when these isotopomers are analyzed in the Casciotti MS (see Appendix B for details).

$^{31}R_{sample}$, $^{45}R_{sample}$, and $^{46}R_{sample}$ values are then entered into the following equations:

$$^{31}R = ((1-\gamma)^{15}R^{\alpha} + \kappa^{15}R^{\beta} + {}^{15}R^{\alpha}{}^{15}R^{\beta} + {}^{17}R(1+\gamma^{15}R^{\alpha} + (1-\kappa)^{15}R^{\beta}))/ (1+\gamma^{15}R^{\alpha} + (1-\kappa)^{15}R^{\beta})$$

$$^{45}R = {}^{15}R^{\alpha} + {}^{15}R^{\beta} + {}^{17}R$$

$$^{46}R = ({}^{15}R^{\alpha} + {}^{15}R^{\beta})\,{}^{17}R + {}^{18}R + {}^{15}R^{\alpha}{}^{15}R^{\beta}$$

$$^{17}R/0.0003799 = (^{18}R/0.0020052)^{0.516}$$



BGD
7, 3019–3059, 2010



where $\gamma$ and $\kappa$ are the yields of the scrambled fragment ions from $^{14}N^{15}NO$ (*m/z* 30) and $^{15}N^{14}NO$ (*m/z* 31) (see Appendix B). The four equations above can be evaluated with a nonlinear equation solver to obtain values for $^{15}R^{\alpha}$, $^{15}R^{\beta}$, $^{17}R$, and $^{18}R$ for each sample.

## Appendix B

### Calculating *m/z* 30 and 31 yield coefficients

When $N_2O$ is introduced into the ion source of the mass spectrometer, some $NO^+$ fragment ions are produced. While most of these ions contain N from the $\alpha$ position, a small amount of "scrambling" occurs, yielding $NO^+$ ions containing the $^{\beta}N$. Accurate measurements of $^{15}R^{\alpha}$ and $^{15}R^{\beta}$ require quantification of the scrambling behavior for the mass spectrometer under standard operating conditions.

Westley et al. (2007) use six separate coefficients to describe the $30^+$ and $31^+$ fragmentation behaviors of the $^{14}N^{15}NO$, $^{15}N^{14}NO$, and $^{15}N^{15}NO$ isotopologues. We followed their recommendation and performed mixing analyses using purified $^{14}N^{15}NO$, $^{15}N^{14}NO$, and $^{15}N^{15}NO$ gases from ICON (Summit, N. J.) to investigate the fragmentation behavior of individual isotopologues in our MS (see supplementary material: http://www.biogeosciences-discuss.net/7/3019/2010/bgd-7-3019-2010-supplement.zip).

We also compared this approach to the results of a simpler approach using two scrambling coefficients, $\gamma$ and $\kappa$, to describe the relative production of *m/z* 30 ions from $^{14}N^{15}NO$ and *m/z* 31 ions from $^{15}N^{14}NO$, respectively. These coefficients were used in the system of equations that convert $^{31}R$, $^{45}R$, and $^{46}R$ to $^{15}R^{\alpha}$, $^{15}R^{\beta}$, $^{17}R$, and $^{18}R$ (see Appendix A for the full set of equations).

We calculated $\gamma$ and $\kappa$ using a series of dual inlet measurements of two sample gases with known isotope and isotopomer ratios referenced to a standard gas that also has a known isotopomer composition. In this case, the sample gases were from the laboratories of K. Koba (Tokyo University of Agriculture and Technology) and N. Ostrom



BGD
7, 3019–3059, 2010



(Michigan State University), and the standard gas was the reference gas from the Casciotti lab (WHOI). These three $N_2O$ reference gases were all calibrated by S. Toyoda (Tokyo Institute of Technology).

For each sample gas the "measured" value of rR 31NO/30NO$_{sample}$/rR 31NO/30NO$_{standard}$ was determined by averaging the results of a series of 10-cycle dual inlet analyses on the Casciotti MS. Then the "calculated" value of rR 31NO/30NO$_{sample}$/rR 31NO/30NO$_{standard}$ (equivalent to $^{31}R_{sample}/^{31}R_{standard}$) was obtained by inserting Toyoda's calibrated values of $^{15}R^{\alpha}$, $^{15}R^{\beta}$, $^{17}R$, and $^{18}R$ for the sample and standard gases into the equation below and guessing values of $\gamma$ and $\kappa$.

$$^{31}R = ((1-\gamma)^{15}R^{\alpha} + \kappa^{15}R^{\beta} + {}^{15}R^{\alpha}{}^{15}R^{\beta} + {}^{17}R(1 + \gamma^{15}R^{\alpha} + (1-\kappa)^{15}R^{\beta}))/$$
$$(1 + \gamma^{15}R^{\alpha} + (1-\kappa)^{15}R^{\beta})$$

The problem is one of optimization where the object is to vary $\gamma$ and $\kappa$ until the calculated values of $^{31}R_{sample}/^{31}R_{standard}$ are as close as possible to the measured rR31/30$_{sample}$/rR31/30$_{standard}$ for both sample gases. This two-coefficient model automatically obeys the constraint of Toyoda and Yoshida (1999) that $\delta^{15}N^{bulk}=(^{15}R^{\alpha}+{}^{15}R^{\beta})/2$. The optimized values used here are $\gamma$=0.1002 and $\kappa$=0.0976. These coefficients are consistent with reported values for fragment ion yields and scrambling coefficients (between 0.08–0.10) (Westley et al., 2007; Toyoda and Yoshida, 1999).

Following the alternative approach of Westley et al. (2007) we found that ionization of the $^{15}N^{14}NO$ ICON standard produced approximately one tenth as many 31 ions as the $^{14}N^{15}NO$ ICON standard (see supplementary material for data and calculations). This result is an independent confirmation of the scrambling coefficient approach described above (because $\kappa/(1-\gamma)$=0.108) and it does not require a priori knowledge of the isotopomeric composition of the reference gas.

For the data presented in this paper, we opted to use two coefficients and assumed that the fragment ion yields of 30 and 31 sum to 1 for both $^{14}N^{15}NO$ and $^{15}N^{14}NO$. Using this approach we were able to reproduce the isotopomer ratio values of sample gases



BGD
7, 3019–3059, 2010



with a broad range of site preferences (calibrated value for P. Ostrom tank=+26.5‰ and the value measured using our approach=+27.0‰; calibrated value of K. Koba tank=−5.4‰ and measured=−4.8‰).

*Acknowledgements.* We would like to thank Sakae Toyoda for calibrating our $N_2O$ reference gas, Robin Sutka and Nathaniel Ostrom for providing the calibrated Michigan State reference gas, and Keisuke Koba for providing the calibrated Tokyo University of Agriculture and Technology reference gas. Marian Westley kindly provided extensive details on her isotopomer intercalibration strategy. Ed Leadbetter suggested the test for heterotrophic denitrification and the high cell density $N_2O$ measurements. Matt McIlvin helped develop the modification necessary to do large-bottle headspace analyses on the MS. Matt First and Mark Dennett provided assistance with the flow cytometer. Alyson Santoro, Cara Manning, and Ed Leadbetter provided suggestions that improved the manuscript immensely.

## References

Alldredge, A. L. and Cohen, Y.: Can microscale chemical patches persist in the sea? Microelectrode study of marine snow, fecal pellets, Science, 235, 689–691, 1987. 3022

Andersson, K. K. and Hooper, A. B.: $O_2$ and $H_2O$ are each sources of one O in $NO_2^-$ produced from $NH_3$ by *Nitrosomonas*: $^{15}$N-NMR evidence, FEBS Letters, 164, 236–240, 1983. 3024, 3036, 3037

Andersson, K. K., Philson, S. B., and Hooper, A. B.: $^{18}$O isotope shift in $^{15}$N NMR analysis of biological N-oxidations: $H_2O$-$NO_2^-$ exchange in the ammonia-oxidizing bacterium *Nitrosomonas*, P. Natl. Acad. Sci., 79, 5871–5875, 1982. 3023, 3036

Arp, D. J., Chain, P. S. G., and Klotz, M. G.: The impact of genome analyses on our understanding of ammonia-oxidizing bacteria, Annu. Rev. Microbiol., 61, 503–528, 2007. 3023

Bard, Y.: Nonlinear Parameter Estimation, Academic Press, New York, 1974.

Beaumont, H. J. E., Hommes, N. G., Sayavedra-Soto, L. A., Arp, D. J., Arciero, D. M., Hooper, A. B., Westerhoff, H. V., and van Spanning, R. J. M.: Nitrite reductase of *Nitrosomonas europaea* is not essential for production of gaseous nitrogen oxides and confers tolerance to nitrite, J. Bacteriol., 184, 2557–2560, 2002. 3023, 3031, 3032, 3033

Beaumont, H. J. E., Lens, S., Reijnders, W. N. M., Westerhoff, H. V., and van Spanning, R.





J. M.: Expression of nitrite reductase in *Nitrosomonas europaea* involves NsrR, a novel nitrite-sensitive transcription repressor, Molecular Microbiol., 54, 148–158, 2004. 3023, 3031, 3032, 3033
Beman, M. J., Arrigo, K. R., and Matson, P. A.: Agricultural runoff fuels large phytoplankton blooms in vulnerable areas of the ocean, Nature, 434, 211–214, 2005. 3021
Bender, M. L.: The $\delta^{18}O$ of dissoved $O_2$ in seawater: a unique tracer of circulation and respiration in the deep sea, J. Geophys. Res.-Oceans, 95, 22243–22252, 1990. 3041
Buchwald, C. and Casciotti, K. L.: Oxygen isotopic fractionation and exchange during bacterial nitrite oxidation, Limnol. Oceanogr., 55, 1064–1074, 2010. 3023
Cantera, J. J. and Stein, L. Y.: Molecular diversity of nitrite reductase genes (*nirK*) in nitrifying bacteria, Environ. Microbiol., 9, 765–776, 2007. 3023
Carlucci, A. F. and McNally, P. M.: Nitrification by marine bacteria in low concentrations of substrate and oxygen, Limnol. Oceanogr., 14, 736–739, 1969. 3022
Casciotti, K. L. and Ward, B. B.: Dissimilatory nitrite reductase genes from autotrophic ammonia-oxidizing bacteria, Appl. Environ. Microbiol., 67, 2213–2221, 2001. 3023
Casciotti, K. L. and Ward, B. B.: Phylogenetic analysis of nitric oxide reductase gene homologues from aerobic ammonia-oxidizing bacteria, FEMS Microbiol. Ecol., 52, 197–205, 2005. 3023
Casciotti, K. L., Sigman, D. M., Hastings, M. G., Bohlke, J. K., and Hilkert, A.: Measurements of the oxygen isotopic composition of nitrate in seawater and freshwater using the denitrifier method, Anal. Chem., 74, 4905–4912, 2002. 3029, 3037
Casciotti, K. L., McIlvin, M., and Buchwald, C.: Oxygen isotopic exchange and fractionation during bacterial ammonia oxidation, Limnol. Oceanogr., 55, 753–762, 2010. 3023, 3024, 3036, 3037, 3040
Casciotti, K. L.: Oxygen isotopes in nitrite: analysis, calibration, and equilibration, Anal. Chem., 79, 2427–2436, 2007. 3029, 3040
Charpentier, J., Farias, L., Yoshida, N., Boontanon, N., and Raimbault, P.: Nitrous oxide distribution and its origin in the central and eastern South Pacific Subtropical Gyre, Biogeosciences, 4, 729–741, 2007, http://www.biogeosciences.net/4/729/2007/. 3033, 3038, 3039
Cline, J. D., Wisegarver, D. P., and Kelly-Hansen, K.: Nitrous oxide and vertical mixing in the equatorial Pacific during the 1982–1983 El Niño, Deep-Sea Res., 34, 857–873, 1987. 3021
Codispoti, L. A. and Christensen, J. P.: Nitrification, denitrification and nitrous oxide cycling in




the eastern tropic south Pacific Ocean, Mar. Chem., 16, 277–300, 1985. 3022
Cohen, Y. and Gordon, L. I.: Nitrous oxide in the oxygen minimum of the eastern tropical North Pacific: evidence for its consumption during denitrification and possible mechanisms for its production, Deep-Sea Res., 25, 509–524, 1978. 3021
Cohen, Y. and Gordon, L. I.: Nitrous oxide production in the ocean, J. Geophys. Res., 84, 347–353, 1979. 3021, 3022
Draper, N. R. and Smith, H.: Applied regression analysis, Wiley, New York, 2 edn., 1981. 3039
Elkins, J. W., Wofsy, S., McElroy, M. B., Kolb, C. E., and Kaplan, W. A.: Aquatic sources and sinks for nitrous oxide, Nature, 275, 602–606, 1978. 3021
Fuhrman, J. A. and Capone, D. G.: Possible biogeochemical consequences of ocean fertilization, Limnol. Oceanogr., 36, 1951–1959, 1991. 3022
Fulweiler, R. W., Nixon, S. W., Buckley, B. A., and Granger, S. L.: Reversal of the net dinitrogen gas flux in coastal marine sediments, Nature, 448, 180–181, 2007. 3021
Galloway, J. N., Schlesinger, W. H., Levy II, H., Michaels, A., and Schnoor, J. L.: Nitrogen fixation: anthropogenic enhancement-environmental response, Global Biogeochem. Cy., 9, 235–252, 1995. 3021
Goreau, T. J., Kaplan, W. A., Wofsy, S. C., McElroy, M. B., Valois, F. W., and Watson, S. W.: Production of $NO_2^-$ and $N_2O$ by nitrifying bacteria at reduced concentrations of oxygen, Appl. Environ. Microbiol., 40, 526–532, 1980. 3021, 3022, 3023, 3030
Hallam, S. J., Mincer, T. J., Schleper, C., Preston, C. M., Roberts, K., Richardson, P. M., and DeLong, E. F.: Pathways of carbon assimilation and ammonia oxidation suggested by environmental genomic analyses of marine *Crenarchaeota*, PLoS Biology, 4, 521–536, 2006. 3023, 3042
Hashimoto, L. K., Kaplan, W. A., Wofsy, S. C., and McElroy, M. B.: Transformations of fixed nitrogen and $N_2O$ in the Cariaco Trench, Deep-Sea Res., 30, 575–590, 1983. 3033
Helder, W. and de Vries, R. T. P.: Estuarine nitrite maxima and nitrifying bacteria (EMS-Dollard estuary), Netherlands Journal of Sea Research, 17, 1–18, 1983. 3033
Hooper, A. B. and Terry, K. R.: Hydroxylamine oxidoreductase of *Nitrosomonas* production of nitric oxide from hydroxylamine, Biochim. Biophys. Acta, 571, 12–20, 1979. 3022
Ignarro, L. J., Fukuto, J. M., Griscavage, J. M., and Rogers, N. E.: Oxidation of nitric oxide in aqueous solution to nitrite but not nitrate: comparison with enzymatically formed nitric oxide from L-arginine, P. Natl. Acad. Sci., 90, 8103–8107, 1993. 3031
Jin, X. and Gruber, N.: Offsetting the radiative benefit of ocean iron fertilization by enhancing





$N_2O$ emissions, Geophys. Res. Lett., 30, 1–4, 2003. 3022
Jorgensen, K. S., Jensen, H. B., and Sorensen, J.: Nitrous oxide production from nitrification and denitrification in marine sediment at low oxygen concentrations, Can. J. Microbiol., 30, 1073–1078, 1984. 3021
Knowles, R., Lean, D. R. S., and Chan, Y. K.: Nitrous oxide concentrations in lakes: variations with depth and time, Limnol. Oceanogr., 26, 855–866, 1981. 3021
Koba, K., Osaka, K., Tobari, Y., Toyoda, S., Ohte, N., Katsuyama, M., Suzuki, N., Itoh, M., Yamagishi, H., Kawasaki, M., Kim, S. J., Yoshida, N., and Nakajima, T.: Biogeochemistry of nitrous oxide in groundwater in a forested ecosystem elucidated by nitrous oxide isotopomer measurements, Geochim. Cosmochim. Acta, 73, 3115–3133, 2009. 3024, 3041
Kool, D. M., Wrage, N., Oenema, O., Dolfing, J., and van Groenigen, J. W.: Oxygen exchange between (de)nitrification intermediates and $H_2O$ and its implications for source determination of $NO_3^-$ and $N_2O$: a review, Rapid Communications in Mass Spectrometry, 21, 3569–3578, 2007. 3023, 3037
Kroopnick, P. and Craig, H.: Oxygen isotope fractionation in dissolved oxygen in the deep sea, Earth Planet. Sci. Lett., 32, 375–388, 1976. 3023, 3041
Laanbroek, H. J., Bar-Gilissen, M.-J., and Hoogveld, H. L.: Nitrite as a stimulus for ammonia-starved *Nitrosomonas europaea*, Appl. Environ. Microbiol., 68, 1454–1457, 2002. 3033
Law, C. S. and Ling, R. D.: Nitrous oxide flux and response to increased iron availability in the Antarctic Circumpolar Current, Deep-Sea Res. II, 48, 2509–2527, 2001. 3022
Levine, N. M., Bender, M. L., and Doney, S. C.: The $\delta^{18}O$ of dissoved $O_2$ as a tracer of mixing and respiration in the mesopelagic ocean, Global Biogeochem. Cy., 23, 1–12, 2009. 3041
Lewis, R. S. and Deen, W. M.: Kinetics of the reaction of nitric oxide with oxygen in aqueous solutions, Chem. Res. Toxicol., 7, 568–574, 1994. 3031
Lipschultz, F., Zafiriou, O. C., Wofsy, S. C., McElroy, M. B., Valois, F. W., and Watson, S. W.: Production of NO and $N_2O$ by soil nitrifying bacteria, Nature, 294, 641–643, 1981. 3031
Mariotti, A., Germon, J. C., Hubert, P., Kaiser, P., Letolle, R., Tardieux, A., and Tardieux, P.: Experimental determination of nitrogen kinetic isotope fractionation: some principles; illustration for the denitrification and nitrification processes, Plant Soil, 62, 413–430, 1981. 3036
McIlvin, M. M. and Altabet, M.: Chemical conversion of nitrate and nitrite to nitrous oxide for nitrogen and oxygen isotopic analysis in freshwater and seawater, Anal. Chem., 77, 5589–5595, 2005. 3028
McIlvin, M. M. and Casciotti, K. L.: Automated stable isotopic analysis of dissolved nitrous oxide



BGD
7, 3019–3059, 2010



at natural abundance levels, Limnol. Oceanogr. Methods, 2010. 3028, 3029
Naqvi, S. W. A., Jayakumar, D. A., Narvekar, P. V., Naik, H., Sarma, V. V. S. S., D'Souza, W., Joseph, S., and George, M. D.: Increased marine production of $N_2O$ due to intensifying anoxia on the Indian continental shelf, Nature, 408, 346–349, 2000. 3021
Nevison, C., Butler, J. H., and Elkins, J. W.: Global distribution of $N_2O$ and the $\Delta N_2O$-AOU yield in the subsurface ocean, Global Biogeochem. Cy., 17, 1–18, 2003. 3022
Nevison, C. D., Weiss, R. F., and Erickson III, D. J.: Global oceanic emissions of nitrous oxide, J. Geophys. Res., 100, 15809–15820, 1995. 3021
Norton, J. M., Klotz, M. G., Stein, L. Y., Arp, D. J., Bottomley, P. J., Chain, P. S. G., Hauser, L. J., Land, Miriam, L., Larimer, F. W., Shin, M. W., and Starkenburg, S. R.: Complete genome sequence of Nitrosospira multiformis, an ammonia-oxidizing bacterium from the soil environment, Appl. Environ. Microbiol., 74, 3559–3572, 2008. 3023
Ostrom, N. E., Russ, M. E., Popp, B., Rust, T. M., and Karl, D. M.: Mechanisms of nitrous oxide production in the subtropical North Pacific based on determinations of the isotopic abundances of nitrous oxide and di-oxygen, Chemosphere-Global Change Science, 2, 281–290, 2000. 3021, 3023, 3024
Ostrom, N. E., Pitt, A., Ostrom, P. H., Grandy, A. S., Huizinga, K. M., and Robertson, G. P.: Isotopologue effects during $N_2O$ reduction in soils and in pure cultures of denitrifiers, J. Geophys. Res., 112, 1–12, 2007. 3041
Pai, S.-C. and Yang, C.-C.: Formation kinetics of the pink azo dye in the determination of nitrite in natural waters, Anal. Chim. Acta, 232, 345–349, 1990. 3027
Payne, W. J., Riley, P. S., and Cox, C. D. J.: Separate nitrite, nitric oxide, and nitrous oxide reducing fractions from *Pseudomonas perfectomarinus*, J. Bacteriol., 106, 356–361, 1971. 3021
Popp, B. N., Westley, M. B., Toyoda, S., Miwa, T., Dore, J. E., Yoshida, N., Rust, T. M., Sansone, F. J., Russ, M. E., Ostrom, N. E., and Ostrom, P. H.: Nitrogen and oxygen isotopomeric constraints on the origins and sea-to-air flux of $N_2O$ in the oligotrophic subtropical North Pacific gyre, Global Biogeochem. Cy., 16, 1–10, 2002. 3021, 3041
Poth, M. and Focht, D.: $^{15}N$ kinetic analysis of $N_2O$ production by *Nitrosomonas europaea*: an examination of nitrifier denitrification, Appl. Environ. Microbiol., 49, 1134–1141, 1985. 3023, 3029, 3032
Remde, A. and Conrad, R.: Production of nitric oxide in *Nitrosomonas europaea* by reduction of nitrite, Arch. Microbiol., 154, 187–191, 1990. 3030, 3031

Ritchie, G. A. F. and Nicholas, D. J. D.: Identification of the sources of nitrous oxide produced by oxidative and reductive processes in *Nitrosomonas europaea*, Biochem. J., 126, 1181–1191, 1972. 3029

Rodionov, D. A., Dubchak, I. L., Arkin, A. P., Alm, E. J., and Gelfand, M. S.: Dissimilatory metabolism of nitrogen oxides in bacteria: comparative reconstruction of transcriptional networks, PLoS Computational Biology, 1, 415–431, 2005. 3031

Schmidt, H.-L., Werner, R. A., Yoshida, N., and Well, R.: Is the isotopic composition of nitrous oxide an indicator for its origin from nitrification or denitrification? A theoretical approach from referred data and microbiological and enzyme kinetic aspects, Rapid Communications in Mass Spectrometry, 18, 2036–2040, 2004. 3024, 3041

Shaw, L. J., Nicol, G. W., Smith, Z., Fear, J., Prosser, J., and Baggs, E. M.: *Nitrosospira* spp. can produce nitrous oxide via a nitrifier denitrification pathway, Environ. Microbiol., 8, 214–222, 2006. 3023

Solorzano, L.: Determination of ammonia in natural waters by the phenolhypochlorite method, Limnol. Oceanogr., 14, 799–801, 1969. 3027

Suntharalingam, P. and Sarmiento, J. L.: Factors governing the oceanic nitrous oxide distribution: simulations with an ocean general circulation model, Global Biogeochem. Cy., 14, 429–454, 2000. 3022

Sutka, R. L., Ostrom, N. E., Ostrom, P. H., Gandhi, H., and Breznak, J. A.: Nitrogen isotopomer site preference of $N_2O$ produced by *Nitrosomonas europaea* and *Methylococcus capsulatus* Bath, Rapid Communications in Mass Spectrometry, 17, 738–745, 2003. 3024, 3025, 3034, 3037, 3038, 3039

Sutka, R. L., Ostrom, N. E., Ostrom, P. H., Gandhi, H., and Breznak, J. A.: Nitrogen isotopomer site preference of $N_2O$ produced by *Nitrosomonas europaea* and *Methylococcus capsulatus* Bath, Rapid Communications in Mass Spectrometry, 18, 1411–1412, 2004. 3024, 3025, 3034, 3037, 3038, 3039

Sutka, R. L., Ostrom, N. E., Ostrom, P. H., Breznak, J. A., Gandhi, H., Pitt, A. J., and Li, F.: Distinguishing nitrous oxide production from nitrification and denitrification on the basis of isotopomer abundances, Appl. Environ. Microbiol., 72, 638–644, 2006. 3024, 3025, 3034, 3037, 3038, 3039

Toyoda, S. and Yoshida, N.: Determination of nitrogen isotopomers of nitrous oxide on a modified isotope ratio mass spectrometer, Anal. Chem., 71, 4711–4718, 1999. 3024, 3045

Toyoda, S., Yoshida, N., Miwa, T., Matsui, Y., Yamagishi, H., and Tsunogai, U.: Production





mechanism and global budget of $N_2O$ inferred from its isotopomers in the western North Pacific, Geophys. Res. Lett., 29, 1–4, 2002. 3024, 3037, 3041

Toyoda, S., Mutobe, H., Yamagishi, H., Yoshida, N., and Tanji, Y.: Fractionation of $N_2O$ isotopomers during production by denitrifier, Soil Biol. Biochem., 37, 1535–1545, 2005. 3023, 3024

Treusch, A. H., Leininger, S., Kletzin, A., Schuster, S. C., Klenk, H.-P., and Schleper, C.: Novel genes for nitrite reductase and Amo-related proteins indicate a role of uncultivated mesophilic crenarchaeota in nitrogen cycling, Environ. Microbiol., 7, 1985–1995, 2005. 3023

Ward, B. B., Olson, R. J., and Perry, M. J.: Microbial nitrification rates in the primary nitrite maximum off southern California, Deep-Sea Res., 29, 247–255, 1982. 3030

Watson, S. W.: Characteristics of a marine nitrifying bacterium, *Nitrosocystis oceanus* sp. nov., Limnol. Oceanogr., 10, R274–R289, 1965. 3025

Westley, M. B., Popp, B. N., and Rust, T. M.: The calibration of the intramolecular nitrogen isotope distribution in nitrous oxide measured by isotope ratio mass spectrometry, Rapid Communications in Mass Spectrometry, 21, 391–405, 2007. 3045

Wrage, N., van Groenigen, J. W., Oenema, O., and Baggs, E. M.: A novel dual-isotope labelling method for distinguishing between soil sources of $N_2O$, Rapid Communications in Mass Spectrometry, 19, 3298–3306, 2005. 3023, 3037

Yoshida, N.: $^{15}N$-depleted $N_2O$ as a product of nitrification, Nature, 335, 528–529, 1988. 3029, 3034

Yoshida, N. and Toyoda, S.: Constraining the atmospheric $N_2O$ budget from intramolecular site preference in $N_2O$ isotopomers, Nature, 405, 330–334, 2000. 3041

Yoshida, N., Morimoto, H., Hirano, M., Koike, I., Matsuo, S., Wada, Eitaro adn Saino, T., and Hattori, A.: Nitrification rates and $^{15}N$ abundances of $N_2O$ and $NO_3^-$ in the western North Pacific, Nature, 342, 895–897, 1989. 3022, 3030, 3034

Yoshinari, T.: Nitrous oxide in the sea, Mar. Chem., 4, 189–202, 1976. 3021

Yung, Y. L. and Miller, C. E.: Isotopic fractionation of stratospheric nitrous oxide, Science, 278, 1778–1780, 1997. 3041



BGD

7, 3019–3059, 2010



**Table 1.** Isotope effects and signatures derived in this paper for *N. marina* C-113a. Best fit values of model parameters for Eq. (6) are given with standard deviations based on covariance estimates in Bard (1974).

| parameter | value | $\sigma$ | description |
|---|---|---|---|
| $^{15}\epsilon_{ND}$ | 57.6‰ | 4.1‰ | N isotope effect of nitrifier denitrification |
| $^{18}\epsilon_{ND}$ | −8.4‰ | 1.4‰ | O isotope effect of nitrifier denitrification |
| $^{18}\epsilon_{NH_2OH}$ | 2.9‰ | 0.8‰ | effective O isotope effect of $NH_2OH$ decomposition |
| $SP_{ND}$ | −10.7‰ | 2.9‰ | site preference of $N_2O$ from nitrifier denitrification |
| $SP_{NH_2OH}$ | 36.3‰ | 2.4‰ | site preference of $N_2O$ from $NH_2OH$ decomposition |



BGD
7, 3019–3059, 2010



**Table 2.** The fraction of $N_2O$ produced by nitrifier denitrification ($F_{ND}$) calculated using measured SP values, Eq. (4b), and the best fit values for $SP_{ND}$ and $SP_{NH_2OH}$ in Table 1.

| density (cells ml$^{-1}$) | 20% $O_2$ | 2% $O_2$ | 0.5% $O_2$ |
|---|---|---|---|
| $2\times10^2$ | 0.26±0.06, $n=5$ | 0.38±0.04, $n=5$ | 0.43±0.09, $n=4$ |
| $2.1\times10^4$ | 0.19±0.03, $n=5$ | 0.18 ± 0.04, $n=5$ | 0.48±0.11, $n=5$ |
| $2\times10^5$ | 0.11±0.03, $n=6$ | – | 0.58±0.11, $n=6$ |
| $1.5\times10^6$ | – | – | 0.87±0.09, $n=5$ |



BGD
7, 3019–3059, 2010



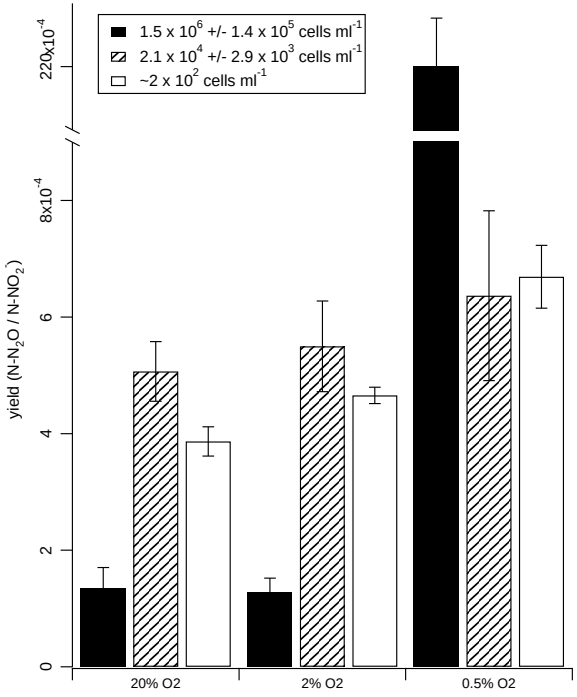


**Fig. 1.** $N_2O$ yields versus cell density. Each bar represents the average of 5 replicate cultures. Error bars are for one standard deviation among replicates.



BGD

7, 3019–3059, 2010



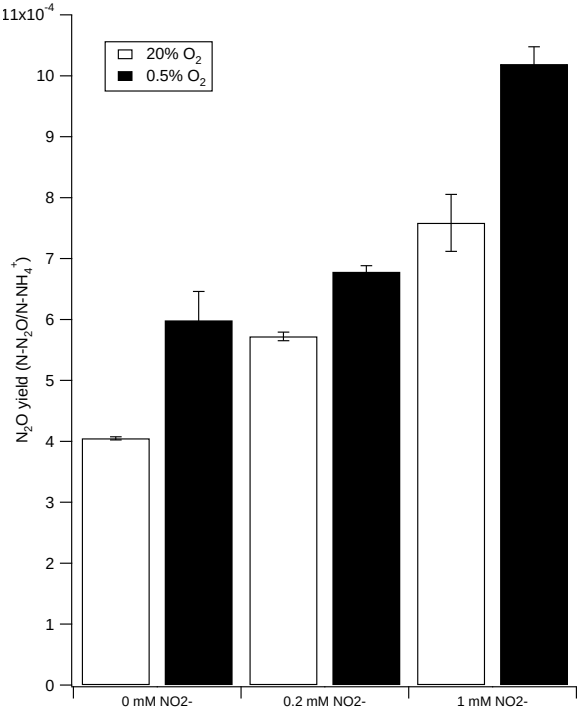


**Fig. 2a.** $N_2O$ yields increased when $NO_2^-$ was added to the starting media. Initial $NH_4^+$ concentrations were 50 µM. Added $NO_2^-$ was either 0, 0.2 mM, or 1 mM.



BGD
7, 3019–3059, 2010



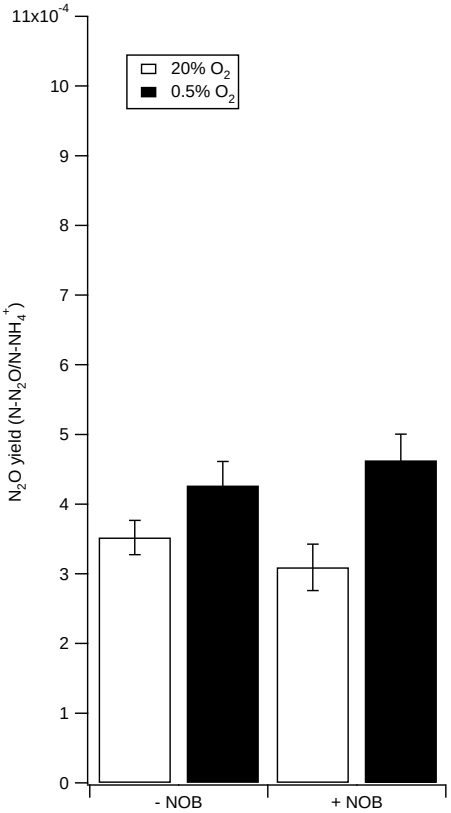


**Fig. 2b.** $N_2O$ yields in the presence and absence of nitrite-oxidizing bacteria. Starting $NH_4^+$ concentrations were 50 µM.



BGD
7, 3019–3059, 2010



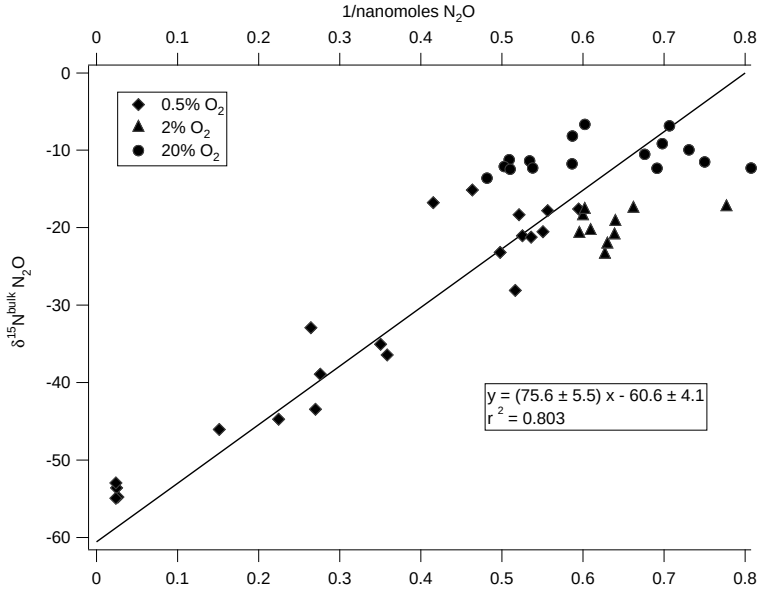


**Fig. 3.** The slope and intercept of a Type II linear regression of $\delta^{15}N^{bulk}$ and 1/mass $N_2O$ regression are given ±one standard deviation. The densities of the cultures represented here were $1.5\times10^6$, $2\times10^5$, $2.1\times10^4$, and $2\times10^2$. In making a linear fit to the data, we assume that any differences in total $N_2O$ are due to nitrifier-denitrification. The y-intercept of the line is equal to the $\delta^{15}N^{bulk}$ of $N_2O$ from nitrifier-denitrification. Data points that were less than 1 nmol $N_2O$ were not included.



BGD

7, 3019–3059, 2010



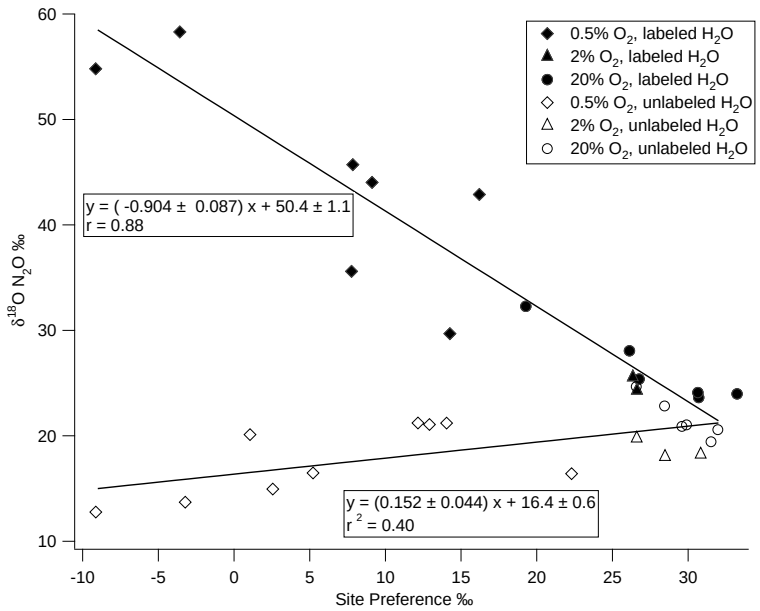


**Fig. 4.** SP and $\delta^{18}$O-$N_2O$ covary. Filled symbols are data from cultures grown in labeled water (about 40‰) and diamonds represent data from cultures in unlabeled water (about −5‰). Regression slopes and intercepts are given ±one standard deviation. The cultures represented here were $1.5\times10^6$, $2\times10^5$, $2.1\times10^4$ cells $ml^{-1}$. Data from cultures that produced less than 1 nmol $N_2O$ were not included. Data from low-density cultures were not included to avoid the impact of relaxation of the $\delta^{18}$O-$NO_2^-$ towards equilibrium with $H_2O$ over the course of the $NH_3$ oxidation reaction. All $\delta^{18}$O values are referenced to VSMOW.



BGD
7, 3019–3059, 2010